

## Article

# Comparison of Satellite and Drone-Based Images at Two Spatial Scales to Evaluate Vegetation Regeneration after Post-Fire Treatments in a Mediterranean Forest

Jose Luis Martinez <sup>1</sup>, Manuel Esteban Lucas-Borja <sup>1</sup>, Pedro Antonio Plaza-Alvarez <sup>1</sup>, Pietro Denisi <sup>2</sup>, Miguel Angel Moreno <sup>3</sup>, David Hernández <sup>3</sup>, Javier González-Romero <sup>1</sup> and Demetrio Antonio Zema <sup>2,\*</sup>

- <sup>1</sup> Escuela Técnica Superior Ingenieros Agrónomos y Montes, Campus Universitario, Universidad de Castilla-La Mancha, E-02071 Albacete, Spain; joseluis.martinez6@alu.uclm.es (J.L.M.); ManuelEsteban.Lucas@uclm.es (M.E.L.-B.); Pedro.Plaza@uclm.es (P.A.P.-A.); Javier.Gromero@uclm.es (J.G.-R.)
- <sup>2</sup> Department AGRARIA, Mediterranean University of Reggio Calabria, Loc. Feo di Vito, I-89122 Reggio Calabria, Italy; pietro.denisi@unirc.it
- <sup>3</sup> Institute of Regional Development, University of Castilla-La Mancha, E-02071 Albacete, Spain; MiguelAngel.Moreno@uclm.es (M.A.M.); David.Hernandez@uclm.es (D.H.)
- \* Correspondence: dzema@unirc.it



**Citation:** Martínez, J.L.; Lucas-Borja, M.E.; Plaza-Alvarez, P.A.; Denisi, P.; Moreno, M.A.; Hernández, D.; González-Romero, J.; Zema, D.A. Comparison of Satellite and Drone-Based Images at Two Spatial Scales to Evaluate Vegetation Regeneration after Post-Fire Treatments in a Mediterranean Forest. *Appl. Sci.* **2021**, *11*, 5423. <https://doi.org/10.3390/app11125423>

Academic Editors: Dario Gioia and Maria Danese

Received: 16 March 2021  
Accepted: 8 June 2021  
Published: 10 June 2021

**Publisher's Note:** MDPI stays neutral with regard to jurisdictional claims in published maps and institutional affiliations.



**Copyright:** © 2021 by the authors. Licensee MDPI, Basel, Switzerland. This article is an open access article distributed under the terms and conditions of the Creative Commons Attribution (CC BY) license (<https://creativecommons.org/licenses/by/4.0/>).

**Abstract:** The evaluation of vegetation cover after post-fire treatments of burned lands is important for forest managers to restore soil quality and plant biodiversity in burned ecosystems. Unfortunately, this evaluation may be time consuming and expensive, requiring much fieldwork for surveys. The use of remote sensing, which makes these evaluation activities quicker and easier, have rarely been carried out in the Mediterranean forests, subjected to wildfire and post-fire stabilization techniques. To fill this gap, this study evaluates the feasibility of satellite (using LANDSAT8 images) and drone surveys to evaluate changes in vegetation cover and composition after wildfire and two hillslope stabilization treatments (log erosion barriers, LEBs, and contour-felled log debris, CFDs) in a forest of Central Eastern Spain. Surveys by drone were able to detect the variability of vegetation cover among burned and unburned areas through the Visible Atmospherically Resistant Index (VARI), but gave unrealistic results when the effectiveness of a post-fire treatment must be evaluated. LANDSAT8 images may be instead misleading to evaluate the changes in land cover after wildfire and post-fire treatments, due to the lack of correlation between VARI and vegetation cover. The spatial analysis has shown that: (i) the post-fire restoration strategy of landscape managers that have prioritized steeper slopes for treatments was successful; (ii) vegetation growth, at least in the experimental conditions, played a limited influence on soil surface conditions, since no significant increases in terrain roughness were detected in treated areas.

**Keywords:** VARI; log erosion barrier; contour-felled log debris; land restoration; vegetation cover

## 1. Introduction

Wildfires can negatively affect soil fertility, biodiversity, land resources, global warming, and human assets; however, positive environmental effects are also recognized, such as increased forest regeneration and nutrient recycling [1]. The Mediterranean ecosystems are adapted to fire disturbance, but the increasing recurrence and high severity of wildfires generate high soil loss and reduce the ability of vegetation to recover [2].

In the Mediterranean Basin, wildfires burn large forest areas not only during summer, but also in mid seasons, when heavy rainstorms may occur [3,4]. For instance, in Spain, even though the number of wildfires has followed a decreasing trend in the last decades [5], wildland is still severely affected by forest wildfires in summer. In the last 10 years, more than 3000 km<sup>2</sup> of forests have burned. Only in 2018, over 7000 wildfires burned about 300 km<sup>2</sup> of forests [5].

The hydrological and ecological effects of large wildfires (floods, landslides and mudslides, erosion, loss of biodiversity, destruction of fauna, etc.) can be devastating [6]. Among these effects, soil erosion is presumably the most severe consequence of forest fires, since it threatens water resources, infrastructures, and populations inside and out of burned areas [7]. For burned soils, erosion after wildfire is much higher compared to unburned, since fire changes several physical and chemical properties of soil [1,7]. For instance, erosion in burned forest areas increases by even 30 times compared to the natural values recorder in unburned zones [8]. To reduce, under tolerable limits, soil erosion, urgent restoration actions are implemented immediately after the wildfire to prevent secondary post-fire damage, whereas long-term restoration can be used for regenerating plants and promoting the evolution of forest structure [9].

Management actions in fire-affected forests have typically focused on soil structure and plant recovery. The increase in vegetal cover through plant regeneration has been identified by some studies in Mediterranean regions as the main driver in post-fire management of forests [10]. Among the post-fire restoration actions, log erosion barriers (hereinafter indicated as “LEB”) or contour-felled log debris (CFD) are widespread measures to control the erosive processes (mainly due to runoff and sediment flows) in forest ecosystems [11]. More specifically, LEBs are built by felling burned trees, while CFDs consist of branch and small-felling burned trees, and both are laid on the ground along the slope contour. Many studies have assessed the effectiveness of hillslope stabilization treatments on soil hydrological response (namely runoff and erosion) (e.g., [12–15]) as well as reductions in CO<sub>2</sub> emissions and carbon sequestration [16]. In some cases, the impact of these actions in reducing runoff and trapping sediments is limited to the less intense rainfall events (e.g., [11]). In other cases, their effects are scarce or negligible, due to inadequate constructions or deficient design [13]. Some studies have even shown a negative impact, in terms of a higher percentage of bare and stony soil, especially in sunny areas subjected to different forest treatments, with subsequent increase in soil erosion [17]. It is evident that the effects of post-fire hillslope treatments are still uncertain, and the most suitable technique has not been completely identified [18].

A monitoring activity of post-fire management actions in burned forests in the Mediterranean environment may give forest managers and landscape planners insight about their effectiveness in reducing soil loss and accelerating the vegetation recovery. This activity is essential, since public administrations make large efforts and spend many resources in restoration actions that usually include economic, cultural and even landscape components [19,20]. However, the techniques of field monitoring are generally expensive and time-consuming [21]. The remote sensing techniques (using satellites and drones) are new tools to make land surveys quicker and cheaper [22]. Remote sensing is usually applied in fire-affected areas for fire risk and fuel mapping, active fire detection, burned area estimates, burn severity assessment, and post-fire monitoring vegetation recovery [23]. The remote sensing techniques using satellite images are able to evaluate post-fire regeneration with increasingly improved spatial, temporal and radiometric resolutions [24]. In the last decade, the appearance of unmanned aerial vehicles has increased the use of remote sensing application to agro-forestry [25,26]. UAV technology is promising for monitoring vegetation regrowth, since the spatial resolution and temporal intervals of surveys are not dependent on satellite orbits [23]. Despite their versatility and low cost, UAVs are not widely used to survey wide areas due to legal and technical limitations (e.g., autonomy, payload capacity) [27]. The assessment of wildfire effects and post-fire regeneration using remote sensing has been done through the calculation of spectral vegetation indices [28]. These indices are calculated using the electromagnetic wave reflectance data of vegetation using passive sensors [29]. Several studies have successfully developed and applied vegetation indices (e.g., the Normalized Difference Vegetation Index, NDVI; the Composite Burn Index, CBI; the Differenced Normalized Burn Ratio, DNBR, and the Visible Atmospherically Resistant Index, VARI [24]. In this regard, Gitas et al. [25] published a comprehensive review about remote sensing of post-fire vegetation recovery and highlighted the impor-

tant role of remote sensing in the future as well as the need to perform more studies in Mediterranean areas. Bhagat et al. [26] reported that UAVs provide data at fine resolution with the desired temporal resolution, which make them cost-effective and efficient data collectors. Regarding satellite images, Sirin et al. [29] was able to compare different multispectral satellite data to assess vegetation cover in abandoned lands and rewetted peatlands. Bright et al. [30] analyzed post-wildfire recovery in different coniferous forest types in North America using the Normalized Burn Ratio (NBR) derived from LandTrendr images. The same index was used in the same environment by Lentile et al. [31] to monitor post-fire burn severity and vegetation response following eight large wildfires. In the Mediterranean Basin, post-fire vegetation recovery was assessed by Bastos et al. [32] in Portugal (using the VEGETATION sensor), Lasaponara et al. [33] in Italy (using satellite MODIS data), and Polycronaki et al. [34] in Greece (using optical and SAR data [35]).

Regarding VARI, several applications have been carried out in different research fields. For example, Schneider et al. [36] showed that VARI outperforms other indexes in distinguishing historical wildfire data in southern California. In the same environment, Stow et al. [37] demonstrated better performances of VARI compared to another normalized index (Normalized Difference Water Index, NDWI) in monitoring chaparral moisture content. Munoz et al. [38] found that VARI was more effective in estimating the fraction of vegetation cover and recognizing the different land use compared to NDVI index, observing a standard error lower than 8%. From these studies, the feasibility of VARI to estimate variable levels of land cover emerges. However, applications of this index for evaluation of vegetation regeneration in fire-affected areas are very scarce. Only Larrinaga and Brotons [39] calculated four greenness indices (among them VARI) to analyze post-fire regeneration of Mediterranean forests. Christakopoulos et al. [40] proposed a comparative evaluation of restoration practices using remote sensing and GIS in naturally-regenerating and reforested areas of Greece. No research is available about the estimation of vegetation recovery after hillslope stabilization techniques using VARI applied to satellite or UAV surveys. This leaves the usability of these methods in post-fire management of forests not well understood, to date.

To fill this gap, the current study evaluates the ability of VARI, estimated by both satellite and UAV images, to quantify the vegetation recovery after post-fire treatments (LEBs and CFDs) in a Mediterranean forest of Central Eastern Spain. Possible correlations between the vegetation cover measured in field plots and VARI values estimated from satellite (LANDSAT8) or UAV images, are identified. Processing of this information at two spatial scales (catchment and hillslope) allows validation of one or both methods.

## 2. Materials and Methods

### 2.1. Study Area

The investigation was carried out in the Sierra de los Donceles (municipality of Hellín, Castilla-La Mancha region, southeast Spain) (Figure 1a,b). This mountain forest lies in the most northeastern part of the Penibetic system with a southeast-northwest aspect. The landscape is patchy with steep slopes (sometimes over 25–30%), predominantly exposed to south-southeast, and ranges between 304 and 808 m above sea level with an average altitude of 506 m.

In this forest, one catchment (hereinafter “catchment area” or “catchment scale”) and one hillslope (“hillslope area” or “hillslope scale”) were selected, both subject to burning and post-fire restoration actions (Figure 1c,d). In these areas, plots for survey of vegetation were installed, as detailed in Section 2.2, and remote sensing-based analysis (using satellite or drone for the catchment and hillslope scale, respectively).

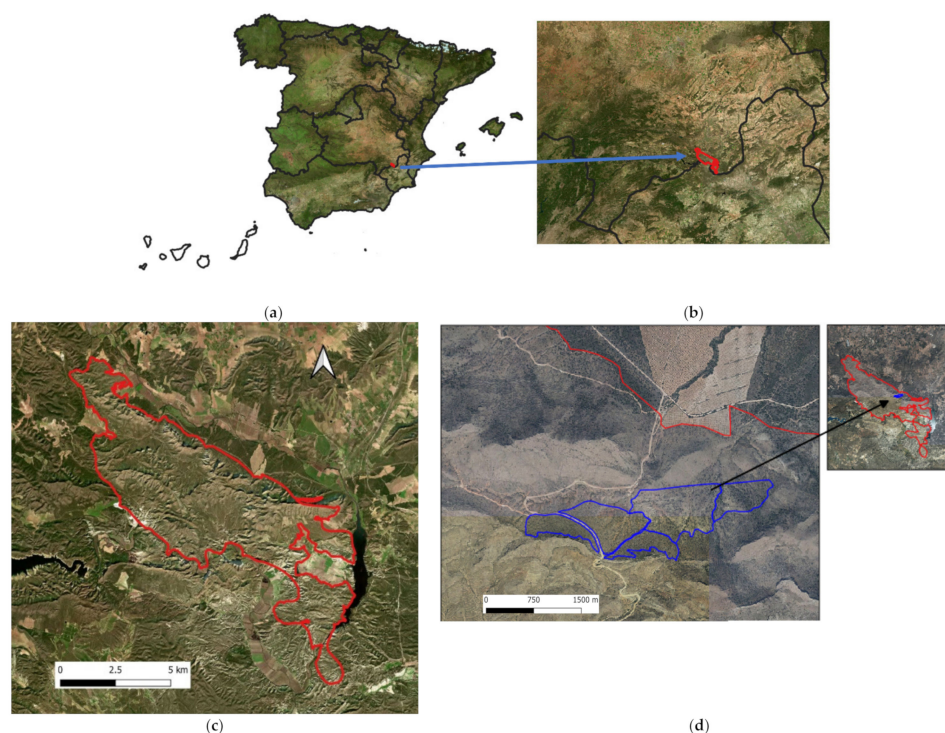


**Figure 1.** Location (a) and aerial map (b) of the study area, catchment area (c) and hillslope area (d) in Sierra de los Donceles forest (Castilla La Mancha, Spain).

The climate of the region is semi-arid Mediterranean. The study area is located in the Mesomediterranean bioclimatic belt [41], which is characterized by a dry climate with scarce rainfalls and a large variability of temperature. The mean annual precipitation is 321 mm and the mean temperature is 16.6 °C (minimum and maximum mean temperatures of −2 and 40 °C, respectively, in February and July (Spanish Agency for Meteorology, AEMET, period of 1981–2010) [42]. According to the Spanish soil map [43], soils belong to the Aridisol order and Calcic suborder, according to the classification established by the Soil Taxonomy System [44].

A large part of the study area is covered by a sclerophyllous vegetation dominated by *Pinus halepensis* Mill forests and with understory mainly consisting of *Quercus coccifera*, *Rhamnus lycioides*, *Halimium hatriplicifolium*, *Rosmarinus officinalis*, *Cistus clusii*, *Rhamnus alaternis*, *Phamnus alaternis*, *Genista spartioides* subsp. *Retamoid*; south-facing areas are dominated by *Stipa spartans* and natural therophytic grasslands. Before the wildfire, tree height and density of *Pinus halepensis* M. were 5 to 12 m and 450 to 775 individuals per hectare, respectively [45]. The wildfire occurred on July 2012, and burned a total area of 6500 ha of forest. The fire propagation was very fast, and most of the land was affected by moderate to high fire severity. After the fire, the Forest Service of Castilla-La Mancha region carried out post-fire restoration works, stabilization treatments on hillslopes (both log erosion barriers and contour-felled log debris) in autumn 2012, and checked dams in the catchment reaches in 2013 (Figure 2b,d and Figure 3).

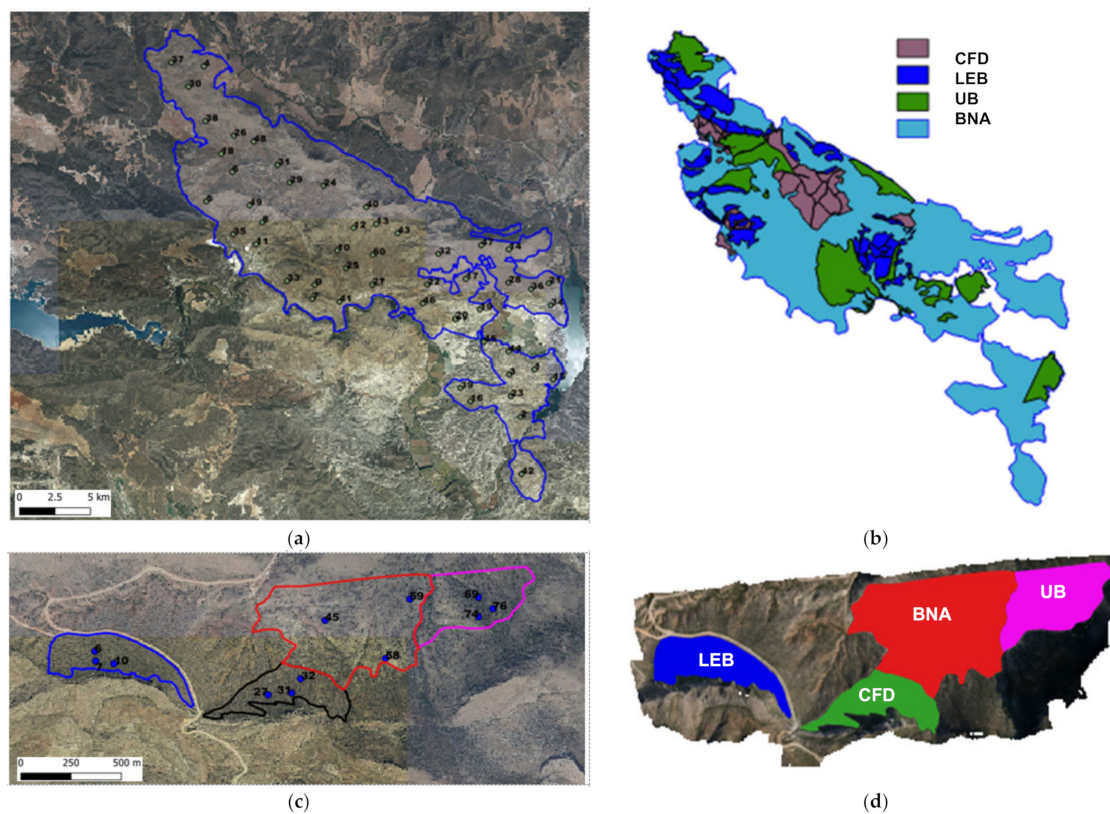


**Figure 2.** Plot location and distribution of soil conditions in the catchment (a,b) and hillslope (c,d) areas in Sierra de los Donceles forest (Castilla La Mancha, Spain). Log erosion barriers (“LEB”), contour-felled log debris (“CFD”), burned and no action (“BNA”), unburned (“UB”).



**Figure 3.** Photos of the construction of contour-felled log debris (a) and log erosion barriers (b) in Sierra de los Donceles forest (Castilla La Mancha, Spain).

## 2.2. Experimental Design

The catchment selected in the studied area was subject to a wildfire and treated with the two hillslope stabilization treatments, consisting of log erosion barriers (“LEB”) and contour-felled log debris (“CFD”) (Figure 3). LEBs were built by felling burned trees that are laid on the ground along the slope contour [46]. Each log was anchored in-place and the space between the log and soil surface was filled with soil to create a storage basin upstream of the LEB, where the water and sediment flows are trapped. Earthen berms were sometimes installed to reduce the share of water circumventing the log sides. In the studied catchment, the stabilization treatment was operated at a mean density of 30 LEBs per hectare with a mean length of 10 m (for a linear density of 300 m of logs per ha). These

densities were limited by the scarce availability of wood material, due to the unsuitable type of vegetation in the area (small-diameter and low-density trees). The CFD treatment consisted of branch and small-felling burned trees, which were laid on the ground along the slope contour, as for LEB. In this case, logs were not anchored. The mean treatment density was 17 CFD per ha with a mean length of 50 m (corresponding to 850 m per ha), given the lower compaction and concentration of the material for building the CFD.

Moreover, a burned area was left without any treatment (henceforth “burned and no action”, BNA) (Figure 2). Another area that was located very close to the burned forest and not affected by fire was considered (“unburned”, UB); the vegetation and soil of this area was extremely similar as those of the burned zone and it was therefore representative of the actual pre-fire conditions. Table 1 reports the vegetation cover in the plots under four land conditions at the two spatial scales.

**Table 1.** Pre-fire forest cover in plots under four land conditions before the wildfire of 2012 in Sierra de los Donceles forest (Castilla-La Mancha, Spain).

| Plot Scale | Land Condition | Forest Cover (%) |
|------------|----------------|------------------|
| Hillslope  | LEB            | 78–84            |
|            | CFD            | 77–81            |
|            | BNA            | 69–75            |
|            | UB             | 77–91            |
| Catchment  | LEB            | 73–84            |
|            | CFD            | 71–79            |
|            | BNA            | 81–87            |
|            | UB             | 78–83            |

Notes: UB = unburned; BNA = burned and no action; CFD = contour-felled log debris; LEB = log erosion barriers; data source: surveys of the Forest Service of Castilla-La Mancha region.

The vegetation cover was characterized in all plots under the four soil conditions. More specifically, in the UB plots, the vegetation cover is mainly characterized by woody and herbaceous species (specifically, *Pinus halepensis*, *Rosmarinus officinalis*, *Brachypodium retusum* and *Cistus albidus*). *Pinus halepensis*, *Cistus albidus* and *Rosmarinus officinalis* can largely be disseminated; their seeds, after fire, are stimulated to germinate. Conversely, *Brachypodium retusum* is a herbaceous species (hemicryptophyte), which is a facultative disseminator, with the ability to reproduce both from sprouts and seed and to adapt to frequent fires. In the BNA plots, *Brachypodium retusum*, *Cistus albidus*, *Halimium halimifolium*, *Quercus coccifera*, *Klasea flavescens* subsp. *cichoracea flubensces* ssp. *leucanta* and *Pinus halepensis* are the main species identified after the wildfire. *Quercus coccifera* is a woody phanerophytic species with vegetative propagation. Most of the area in the CFD plots was covered after the wildfire by species with different strategies of fire response, mainly seeding trees (*Cistus albidus*, *Fumana ericoides*, *Pinus halepensis*), but also sprouting (*Rhamnus lycioides*, *Pistacia lentiscus*) and facultative sprouting (*Anthyllus cytisoides*) trees as well as facultative sprouting herbaceous species (*Brachypodium retusum*). Finally, also in LEB plots, we surveyed, after the wildfire, a variety of species with different response strategies to the fire. Woody seeding species prevail (*Fumana helicoide*, *Cistus albidus*, *Rosmariuns officinalis*, *Pinus halepensis*, *Atriplex halimus*), but also woody sprouting trees (*Rhamnus lycioides*, *Juniperus oxycedrus*), woody facultative sprouting (*Retama sphaerocarpa*), herbaceous facultative sprouting (*Brachypodium retusum*, *Macrochloa tenacissima* (L.) Kunth), and herbaceous seeding (*Asphodelus fistulosus*) species.

### 2.3. Data Collection and Processing

#### 2.3.1. Field Survey of Vegetation Cover

Four years after the fire (in the summer of 2016), fifty 30 m × 30 m plots were established in the catchment area (Figure 2a,b) and installed in each of the four land conditions (7 plots in LEB, 7 in CFD, 25 in BNA, and 11 in UB). An additional twelve

10 m × 10 m plots were installed in the hillslope area (Figure 2c,d) for the same land conditions (3 plots in LEB, 3 in CFD, 3 in BNA, and 3 in UB), totaling 62 sample plots (Figure 2c,d). All the plots were separated 100 m from each other, to be considered as independent; moreover, the burned plots were exposed to similar fire severity. In each plot, three strips were selected (10 m long and 0.5 m wide for the 10 m × 10 m plots, and 30 m long and 0.5 m wide for the 30 m × 30 m plots), where the vegetation cover was measured in percentage. Along each strip, we identified the different species, and calculated the percent canopy cover by the line intercept method [46] as the sum of canopy distances by the strip length. The data were averaged in plot as the mean of the three strips [47,48].

### 2.3.2. Remote Sensing Surveys of Vegetation Cover

On the plots at the hillslope scale, in 2016, a scheduled drone flight was carried out. The UAV used was a quadcopter md4-1000 (Microdrones Inc., Kreuztal, Germany) with a RGB SONY ILCE-5100 digital camera (Sony Corporation, Tokyo, Japan) on board. The sensor of the SONY ILCE-5100 camera was a complementary metal oxide semiconductor (CMOS) Exmor<sup>®</sup> type APS-C (23.5 × 15.6 mm) with pixel size of 4 × 4 μm. The image size was 6000 × 4000 (columns and rows) and its focal length was 20 mm. Flight planning was performed for a flight altitude of 120 m obtaining a ground sample distance (GSD) of 0.015 m (Figure 4). LANDSAT8 images of the same date were collected over the plots at the catchment scale (Figure 4). *VARI* values were calculated using UAV and LANDSAT8 images, both from 2016. LANDSAT image was subjected to atmospheric correction and radiometric calibration [49] without using LEDAPS approach. *VARI* was calculated for each pixel, which identifies the vegetation in the part of the visible spectrum (ideal for RGB images). *VARI* is calculated as follows [24]:

$$VARI = \frac{Green - Red}{Green + Red - Blue} \quad (1)$$

Once calculated, *VARI* was then classified, splitting the entire range of data into five classes, to which a “rank” was given for both image sources (satellite and UAV) (Table 2). Then, possible correlations between the *VARI* values and the vegetation cover measured in the plots in 2016 at the two spatial scales were found. Using the *VARI* values, the effects of the land restoration measures on the vegetation cover in comparison with the burned and not treated, as well as to the unburned land, were evaluated.

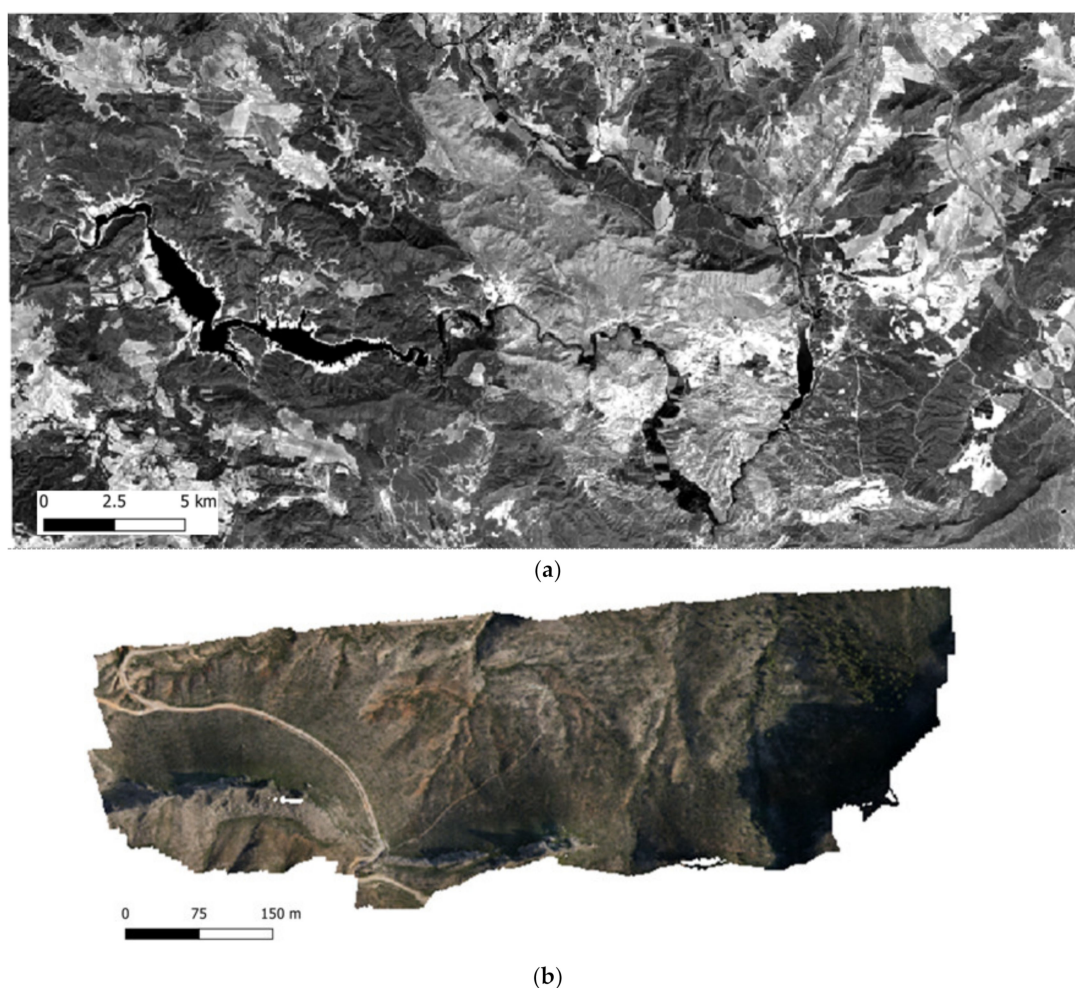


**Figure 4.** Examples of satellite (a) and drone (b) images caught in Serra de Los Donceles forest (Castilla-La Mancha, Spain).

**Table 2.** Calculation of the class width for the VARI classification in ranks in Sierra de Los Donceles forest (Castilla-La Mancha, Spain) (Source: our processing).

| VARI                  | LANDSAT8 | UAV    |
|-----------------------|----------|--------|
| Minimum               | −0.215   | −0.599 |
| Maximum               | 0.058    | 0.173  |
| Range                 | 0.273    | 0.771  |
| Class width (range/5) | 0.055    | 0.154  |

#### 2.4. Spatial Analysis

Using QGIS software applied to a digital terrain model (DTM) prepared by the Spanish Center of Geographic Information in 2016 (resolution of  $5 \times 5$  m), a spatial analysis was carried out to calculate the values of land slope and terrain roughness at the hillslope scale. As exposed by Wu et al. [50], terrain roughness is defined as the unevenness of the terrain surface (including rocks and low vegetation) at scales of several meters. This analysis was targeted to identify possible relationships between vegetation regeneration and land characteristics (that is, land slope and terrain roughness) for the different soil conditions. In order to analyze VARI index and its relationships with land slope and terrain roughness at the hillslope scale, a total of 100 plots were randomly selected on the DTM prepared by the Spanish Center of Geographic Information in 2016 (40 plots in LEB, 20 in CFD, 20 in BNA, 20 in UB).

### 2.5. Statistical Analysis

For both field measurements and remote sensing estimations, General Linear Models (GLM, using treatment as fixed factor and plot as random factor) was applied to evaluate the statistical significance of the differences in the vegetation cover or VARI among the treatments and the control areas. This statistical approach allows us to deal with pseudo-replication [51]. The homogeneity of the variance and the normality of the samples were checked using the Levene and Kolmogorov-Smirnov tests, respectively. All plots were considered spatially independent. The independent Fisher's least significant difference (LSD) test was used for post hoc comparisons. An  $\alpha$ -level  $<0.05$  was adopted. Finally, linear correlations were calculated between VARI and vegetation cover measured in field surveys on one side, as well as land slope and terrain roughness on the other side.

## 3. Results and Discussion

### 3.1. Field Measurements of Vegetation Cover in Different Land Conditions

All surveyed plant species of this study were typical of post-fire vegetation succession in the Mediterranean forest. These species are commonly found in open areas receiving high solar radiation and adapted to fire through different vegetative and reproductive mechanisms. In more detail, the floristic composition of the shrub and herbal layer in the surveyed area was not significantly altered by fire. In fact, the species that have repopulated the forest areas after fire belonged to the pre-existing populations. The number of species did not change, since after the fire, the species progressively regenerates, thanks to the adaptation to new conditions of light, water and nutrients.

The vegetation cover measured in the plots under the four land conditions was more extensive in the areas treated with LEB (vegetal cover of  $84.5 \pm 4.5\%$ ) compared to CFD plots ( $76.9 \pm 5.6\%$ ). As expected, the extreme values were surveyed in UB (100%) and BNA ( $65.5 \pm 4.2\%$ ) (Figure 5). These differences were significant after one-way ANOVA ( $p < 0.05$ ), except for LEB treatment (not significantly different from UB and CFD). According to fieldwork and forest regional managers, this change is mainly due to shrub regeneration and growth. The Mediterranean vegetation is highly adapted to wildfires and these ecosystems are able to respond to fire using resprout or seeding mechanisms. That change is attributed to the higher biomass of the scrub and herbal layer. As recently stated by Keeley and Pausas [52], fire does not threaten ecosystem health, since it is a necessary process and a natural disturbance that is beneficial for the functionality of a fire-adapted ecosystem in Mediterranean forests. As demonstrated by our results, following fire disturbance, Mediterranean forests can regenerate from seed banks stored in soils and basal resprouts.

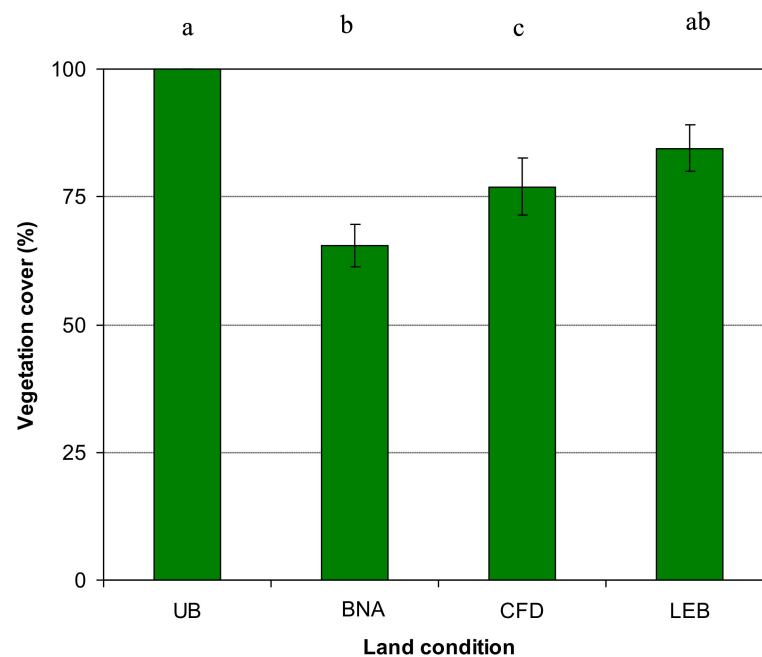
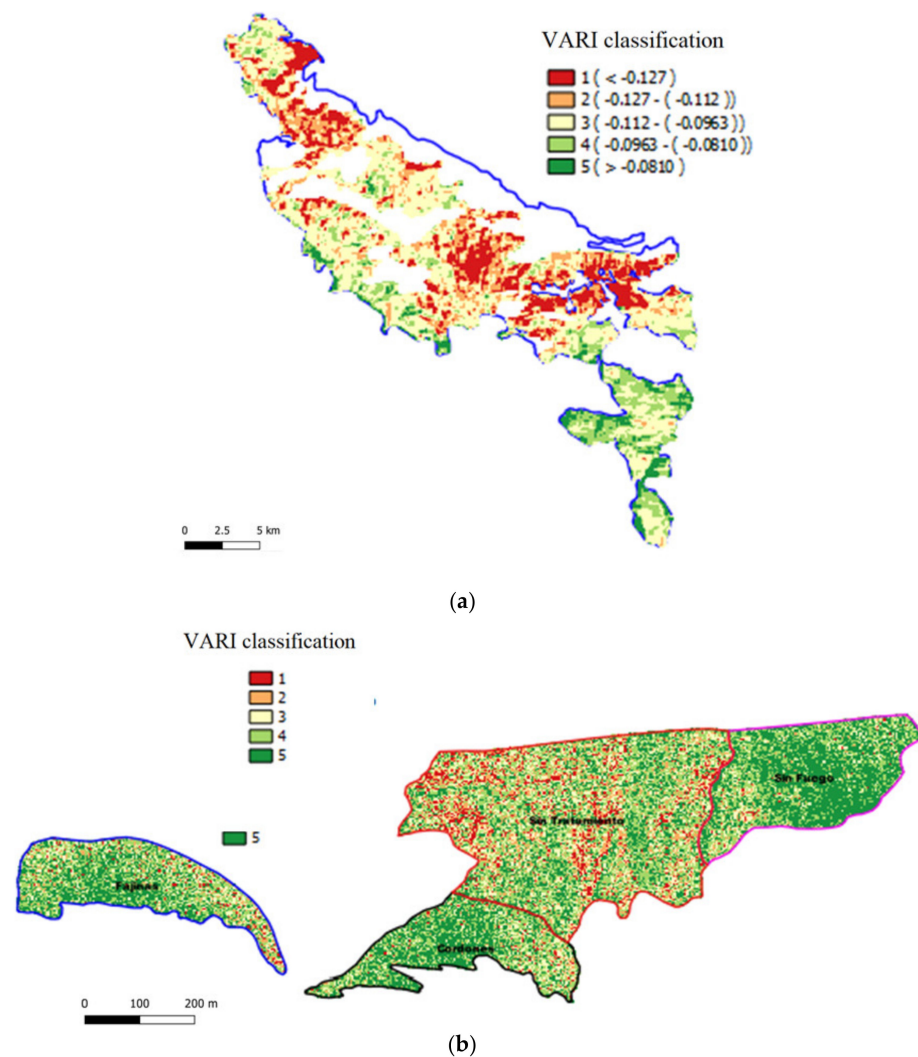


**Figure 5.** Vegetation cover (mean  $\pm$  standard deviation of 62 plots) in plots under four land conditions (UB = unburned; BNA = burned and no action; CFD = contour-felled log debris; LEB = log erosion barriers) after the wildfire of 2012 in Sierra de Los Donceles forest (Castilla-La Mancha, Spain). Mean values that do not share a lower case letter (top of graph) are significantly different from each other (HSD,  $p < 0.05$ ).

This means that, four years after the wildfire, the vegetation regeneration is far from covering the entire area, such as in the unburned zone. The implementation of post-fire treatments allows for a significantly faster recovery process, and LEBs are particularly effective. This higher regeneration compared to CFD-treated areas is somewhat expected, since the dead and burned material of which CFDs consist of is degrading, as well as incorporated more easily compared to the burned wood of LEBs [53]. Both post-fire management techniques are recognized to reduce runoff and erosion (by slowing flows of water and sediments) [14] and improve the physico-chemical properties of soils (increasing infiltration and water retention, and organic matter and nutrients), thus enhancing establishment and development of vegetation [12]. Some LEBs can trap up to 40% of sediments; moreover, this treatment is cheaper compared to other hillslope stabilization techniques [54]. CFDs are effective to reduce water and sediment flows in burned forest subject to machinery salvage logging [55]. Moreover, according to Badía et al. [13], hillslope stabilization after wildfire is a physical barrier that avoids losses or reductions in soil organic matter and nutrients. At the same time, logs of CFDs and canopy residues of LEBs can change the microclimate and land conditions, as well as represent organic matter source after decomposition. This enhances the biological activity of soils [18]. Moreover, decreased evaporation, higher soil moisture, and soil organic matter accumulation upslope of LEB and CFD might lead to an increase in soil respiration and microbial activity, also enhancing nutrient availability after a burn at 5 years from the wildfire). Regarding other studies evaluating post-fire regeneration of vegetation, Christakopoulos et al. [40] found that reforestation was, in some cases, comparable, and in other areas, higher, compared to natural regeneration of pines in burned forests of Greece.

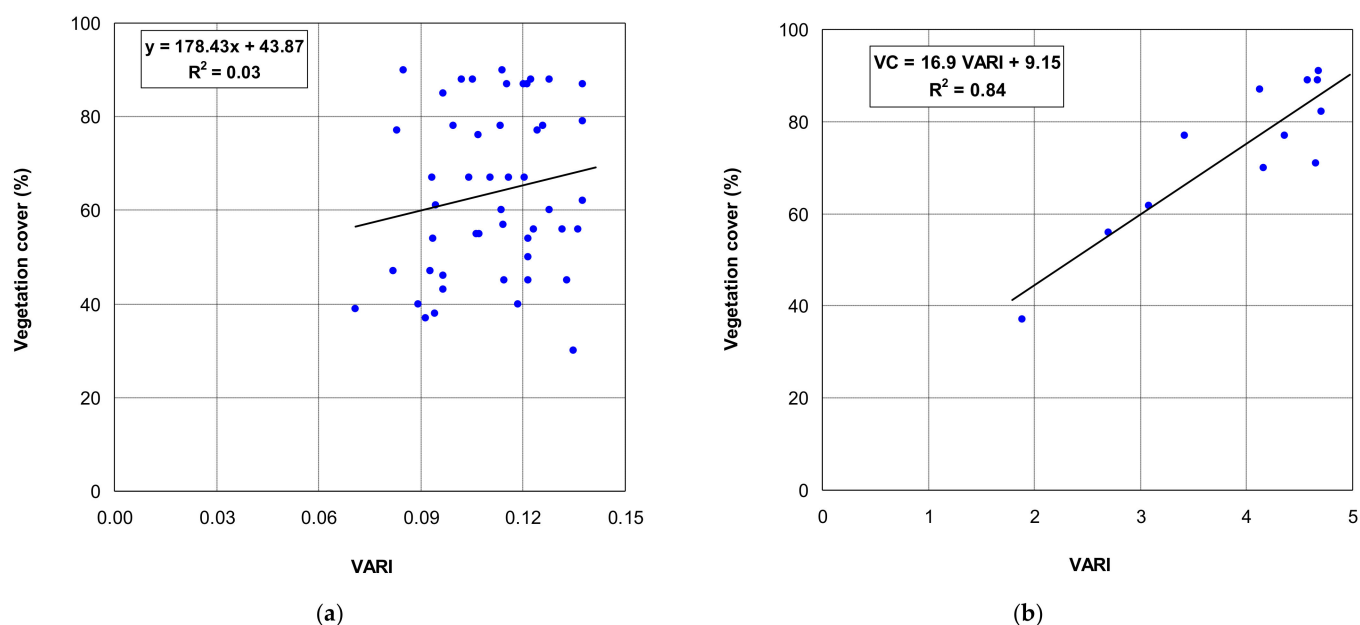
### 3.2. Correlations of VARI with Vegetation Cover Using Remote Sensing Techniques

Figure 6a,b reports the maps of VARI distribution in the experimental areas at both catchment and hillslope scales. In particular, Figure 6b highlights that VARI is higher in the areas subjected to post-fire treatments and lower in burned and untreated land.



**Figure 6.** Spatial distribution of VARI surveyed by satellite (a) and UAV (b) images of 2016 among four land conditions after the wildfire of 2012 in Sierra de Los Donceles forest (Castilla-La Mancha, Spain). Legend: Fajinas = log erosion barriers; cordones = contour-felled log debris; sin tratamiento = burned and no Action; sin fuego = unburned.

A low and not significant  $R^2$  (0.03,  $p > 0.05$ ) was found regressing the LANDSAT8-derived VARI with the vegetation cover measured in field (Figure 7a, catchment scale), while the regression of UAV-derived VARI versus vegetation cover was significant ( $R^2 = 0.84$ ,  $p < 0.05$ ) (Figure 7b, hillslope scale). This difference is clearly due to the lower spatial resolution of satellite data compared to surveys by UAV.



**Figure 7.** Correlations between VARI and vegetation cover at catchment (a), and hillslope (b) scales surveyed by LANDSAT8 and UAV images (2016) in Sierra de Los Donceles forest (Castilla-La Mancha, Spain).

The regression equations for the correlation VARI versus vegetal cover (VC) measured in field was the following:

$$VC = 16.90 \text{ VARI} + 9.15 \quad (2)$$

The vegetation cover distribution in classes according to the VARI classification by UAV is reported in Table 2 and confirms the spatial differences among the land conditions. By visually comparing the vegetation cover distribution according to the two VARI classifications (satellite and UAV, Table 2), no overlap among the same class was detected. This lack of correspondence further confirms the higher reliability of VARI estimated from UAVs to reproduce land cover compared to estimations by satellite, due to unsuitability of image resolution.

The use of VARI to evaluate vegetation regeneration from UAVs has been widely studied in literature. To cite the most recent studies, VARI was used to analyze vegetation on different land uses (e.g., [36–39,56]), monitoring vegetation into water bodies (e.g., [57]), and preparation of the Digital Elevation Model (DEM) [58]). This index shows significant correlation with crop height and yield [59,60]. In burned lands, Larrinaga and Brotons [39] calculated VARI for analysis of post fire regeneration of Mediterranean forests. However, these authors reported that this index underperformed compared to other greenness indexes, such as the Excess green index (ExGI) and green chromatic coordinate (GCC) index, and the same was found for the green red vegetation index (GRVI). Despite this, these authors have demonstrated that low-cost UAVs may improve forest monitoring after disturbance, even in those habitats and situations where resource limitation is an issue. In general, VARI shows a minimal sensitivity to atmospheric effects [26,61,62].

### 3.3. Evaluation of the Vegetation Regeneration in Fire-Affected and Treated Areas Using VARI

The comparison of the mean VARI values under the four studied land conditions between the two remote images shows that, at the catchment scale, VARI was higher ( $0.009 \pm 0.046$ ) under CFDs and lower ( $-0.034 \pm 0.035$ ) in UB areas. This appears again unrealistic, further confirming the misleading meaning of land cover images captured by UAV. Moreover, the differences among the four land conditions were not significant ( $p = 0.724$ ) (Figure 8a).

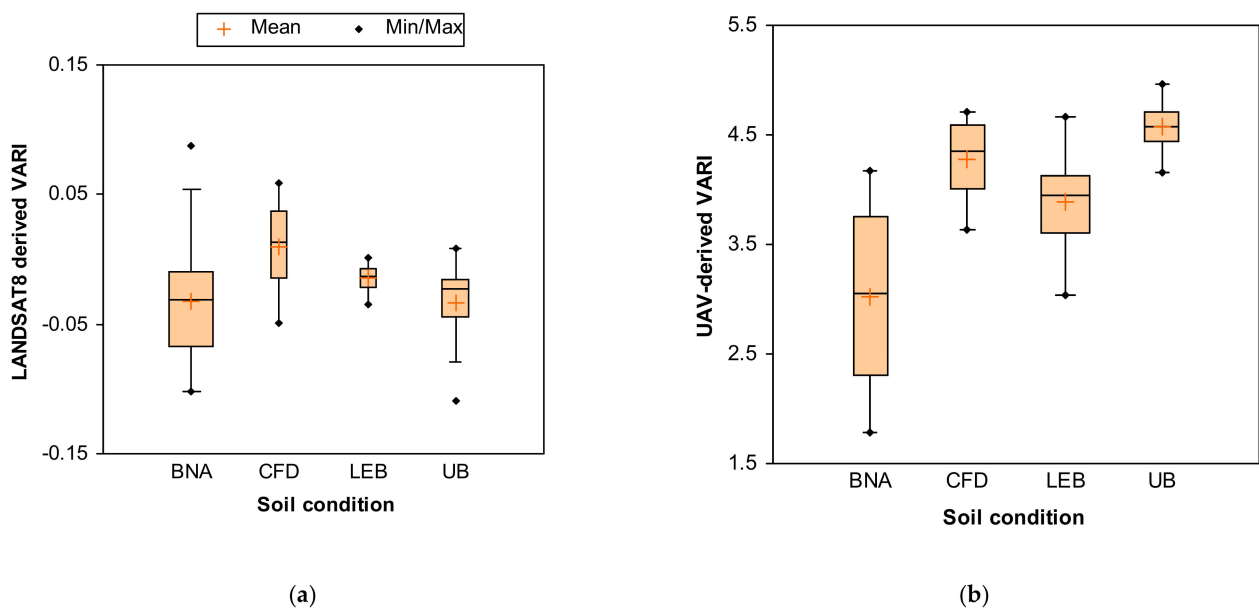


**Figure 8.** Mean values of VARI surveyed by LANDSAT8 (a) and UAV (b) images (2016) among four land conditions after the wildfire of 2012 in Sierra de Los Donceles forest (Castilla-La Mancha, Spain).

In contrast, when analyzing the images by UAV, the highest VARI ( $4.578 \pm 0.230$ ) was found in the UB areas (indicating the most extensive vegetation cover), while the lowest value was detected in the areas burned but not treated (VARI of  $3.024 \pm 0.853$ ). However, in contrast with field surveys, vegetation regeneration was higher in the land treated with CFDs (mean VARI of  $4.270 \pm 0.350$ ) compared to the areas with LEBs ( $3.889 \pm 0.416$ ) (Figure 8b). As for field surveys, the differences in VARI were significant ( $p < 0.05$ ) at this smaller scale using the UAV. Lack of correspondence between the post-fire land treatments suggests that UAV is a viable technique in detecting the variability of vegetation cover only when the difference in VARI mean values is noticeable (e.g., between burned and unburned areas); conversely, the contrasts between areas with similar VARIs may be quite misleading, for instance, when the effectiveness of a treatment has to be evaluated. This result is in close accordance with the indications by Corona et al. [63], who suggested the use of aerial and satellite imagery characterized by high or, better, very high spatial resolution for an effective support to post-fire management (burned area mapping, fire severity assessment, post-fire vegetation monitoring).

Comparisons to other published data about evaluations of post-fire vegetation recovery using remote sensing and greenness indices reveal that SAR images perform better compared to optical images in estimating forest regeneration, particularly when object-based classification procedure is applied (nearly 90% of accuracy) [34]. Moreover, Lasaponara et al. [33] found a better reliability of NDVI (Normalized Difference Vegetation Index) in capturing the diverse vegetation regeneration in both natural and managed areas as well as before and after fire occurrence compared to NBR index, thanks to the data processing using detrended fluctuation analysis (DFA). LANDSAT time series analysis with NBR application was a useful means of describing and analyzing post-fire vegetation recovery across mixed-severity wildfire extents [30], while, in contrast, Lentile et al. [31] reported that dNBR is an imperfect indicator of post-fire effects on vegetation and soil, when the burned areas are affected by different burn severities and are of a highly variable patch size. Regarding the use of drone images, Fernández-Guisuraga et al. [64] highlighted the more detailed spatial information provided by the drone orthomosaic compared to WorldView-2 satellite imagery in vegetation regeneration of heterogeneous burned areas.

Overall, the use of UAV systems for vegetation recovery monitoring is still under development, since these systems have a great potential not yet fully valorized; however,

this use is still limited by some constraints, such as battery life and availability of cameras with suitable spectral range, as well as cost [22].

### 3.4. Spatial Distribution of Land Slope and Roughness, and Correlations with VARI

The spatial analysis carried out in the experimental areas showed that the slope of land subjected to post-fire treatments was significantly different ( $32.2 \pm 5.26\%$  for LEB and  $36.2 \pm 2.61\%$  for CFD) compared to the BNA ( $23.1 \pm 6.22\%$ ), but similar to the UB land ( $36.6 \pm 3.71\%$ ) (Table 3 and Figure 9a). This may be due to the fact that landscape managers prioritized steeper areas when post-fire treatments were planned, since the zones with higher slopes are more prone to erosion and hydrogeological risks compared to flat areas.

**Table 3.** Values (mean  $\pm$  standard deviation) of land slope and terrain roughness in the small-scale areas under four land conditions in Sierra de los Donceles forest (Castilla-La Mancha, Spain).

| Treatment | Land Slope (%)    | Terrain Roughness ( $\mu\text{m}$ ) |
|-----------|-------------------|-------------------------------------|
| LEB       | $32.2 \pm 5.26$ a | $0.08 \pm 0.03$ a                   |
| CFD       | $36.2 \pm 2.61$ a | $0.09 \pm 0.01$ a                   |
| BNA       | $23.1 \pm 6.22$ b | $0.06 \pm 0.03$ a                   |
| UB        | $36.6 \pm 3.71$ a | $0.28 \pm 0.21$ b                   |

Notes: UB = unburned; BNA = burned and no action; CFD = contour-felled log debris; LEB = log erosion barriers; different lower case letters indicate significant differences (HSD,  $p < 0.05$ ).

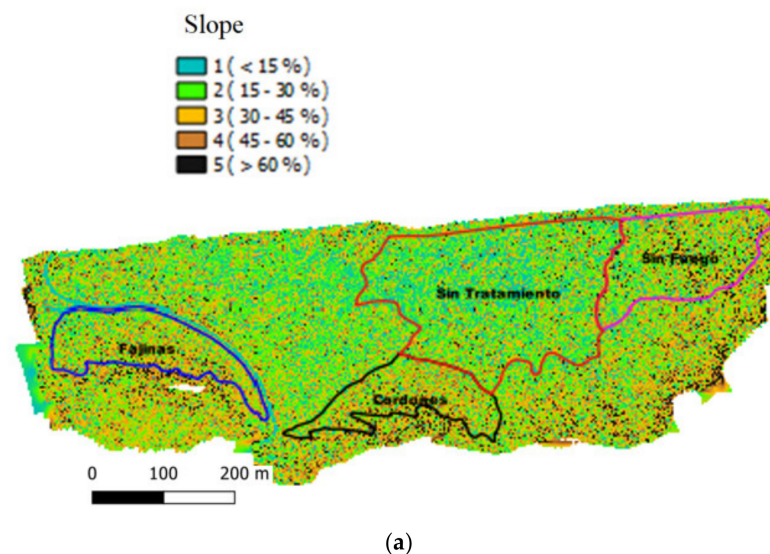


**Figure 9.** Cont.

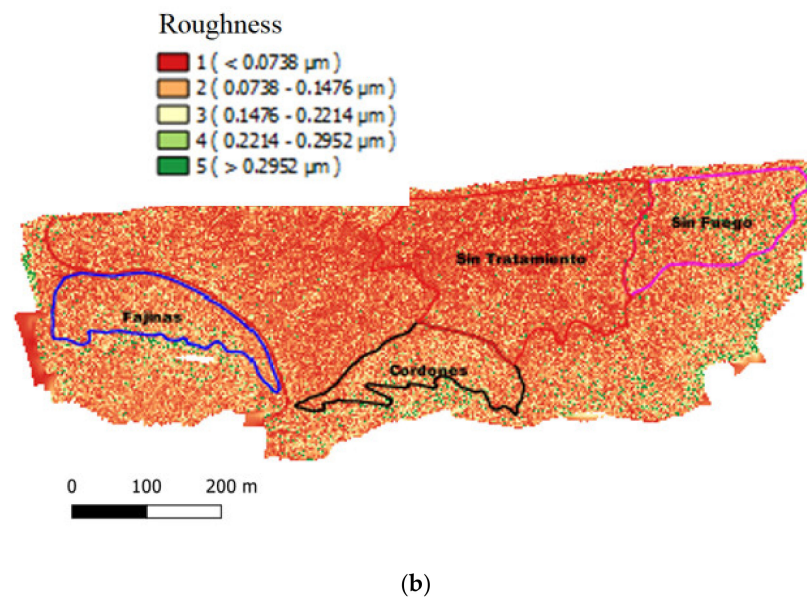


**Figure 9.** Spatial distribution of land slope (a) and terrain roughness (b) surveyed by UAV images of 2016 among four land conditions after the wildfire of 2012 in Sierra de Los Donceles forest (Castilla-La Mancha, Spain). Legend: Fajinas = log erosion barriers; cordones = contour-felled log debris; sin tratamiento = burned and no action; sin fuego = unburned.

According to the land map of Figure 9b prepared using spatial analysis, the terrain roughness of the burned areas was significantly different ( $0.08 \pm 0.03 \mu\text{m}$  for LEB,  $0.09 \pm 0.01 \mu\text{m}$  for CFD, and  $0.06 \pm 0.03 \mu\text{m}$  for BNA) compared to UB zone ( $0.28 \pm 0.21 \mu\text{m}$ ) (Table 2). This means that the vegetation growing in the burned and treated zone do not have a significant effect on the terrain roughness compared to the area without treatment, and that these values are well below the roughness of the unburned soil. A high terrain roughness is beneficial to reduce surface runoff and thus, sediment transport downstream [65–67]. Soil preparation (e.g., by tillage, conditioning, and terracing) after wildfire may be suggested, in order to enhance vegetation growth and improve the soil's resistance to erosion [68–71].

A fair and significant linear correlation was found regressing VARI on land slope under all soil conditions ( $r^2 = 0.52$ ,  $p < 0.05$ ) (Figure 10a), while the linear regression between VARI and terrain roughness was much lower ( $r^2 = 0.15$ ) and not significant ( $p = 0.49$ ) (Figure 10b). This correlation becomes significant ( $p < 0.05$ ) although, again, low ( $r^2 = 0.35$  to  $0.38$ ), adopting exponential or logarithmic equations, whose physical meaning is, however, difficult to be justified (data not shown).

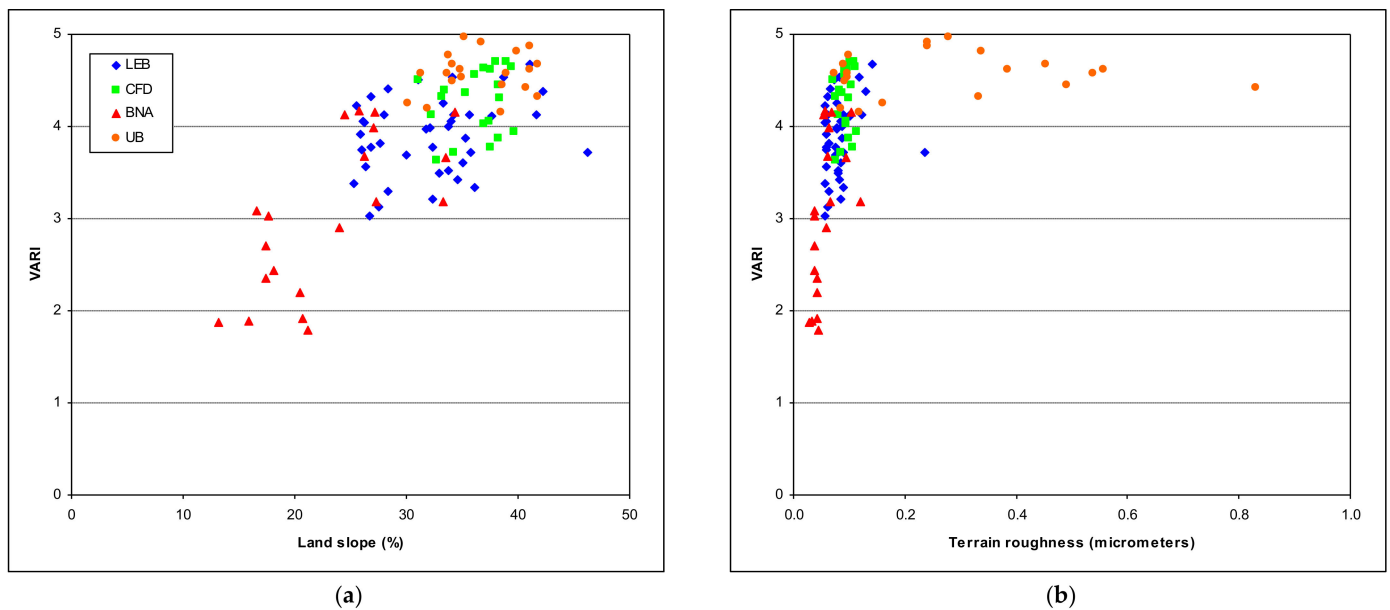


**Figure 10.** Scatterplots of vegetation regeneration (measured by VARI by UAV images of 2016) versus land slope (a) and terrain roughness (b) among four land conditions after the wildfire of 2012 in Sierra de Los Donceles forest (Castilla-La Mancha, Spain).

The first correlation suggests that the effectiveness of post-fire treatments on vegetation regeneration (measured using VARI) increased with slope, and thus, the strategy of landscape managers that have prioritized steeper slopes for treatments was successful. By contrast, the lower, or absence of, significance of correlations between VARI and terrain roughness implies that vegetation growth, at least in the experimental conditions, played a limited influence on soil surface conditions. However, vegetation regeneration remains a key factor to reduce soil exposure to erosion in wildfire-affected areas.

#### 4. Conclusions

The surveys of vegetation cover using fieldwork and remote sensing in lands burned by wildfire in a Mediterranean forest showed that:

- Post-fire treatments improve the vegetation regeneration compared to the burned and not treated areas (by about 20% for CFDs and 30% for LEBs); in this sense, the post-fire treatment using LEBs appears to be more promising compared to the CFD technique;
- Surveys by UAV are useful to detect the variability of vegetation cover among burned and unburned areas through VARI, but may be unrealistic when the effectiveness of a post-fire treatment must be evaluated;
- LANDSAT8 images are less reliable to evaluate the land cover post-fire treatments, due to the lack of correlation between VARI and vegetation cover, and may be because of the resolution that is not suitable for small plants.

The spatial analysis of distribution of VARI and land characteristics at the hillslope scale proved that:

- The post-fire restoration strategy of landscape managers that have prioritized steeper slopes for treatments was successful;
- Vegetation growth, at least in the experimental conditions, played a limited influence on soil surface conditions, since no significant increases in terrain roughness were detected in treated areas.

However, the validity of these preliminary results must be confirmed in other experimental conditions, such as in areas with different climate and soil conditions, as well as in soils subjected to other post-fire management techniques. The effects of patch vegetation should be also explored, since a high spatial variability of vegetation may not be fully cap-

tured by aerial or satellite images. Additionally, the implementation of UAV-based surveys throughout the different stages of vegetation regeneration after wildfire can be suggested, in order to develop a viable tool for monitoring the effectiveness of post-fire techniques over time. A wider validation activity should ensure a practical use of UAV images to support the activity of land managers in planning and implementing efficient measures to restore wildfire-affected areas using vegetation cover. The research question about the viability of higher-resolution satellite images to detect contrasts in vegetation cover among different land conditions remains open. Presumably, the integration of several techniques, combining advantages and limiting constraints, can be suggested for estimation of post-fire vegetation recovery in forest ecosystems with dynamically variable characteristics.

**Author Contributions:** Conceptualization, M.E.L.-B. and P.A.P.-A.; methodology, M.E.L.-B., M.A.M., D.H., J.G.-R., D.A.Z., and P.A.P.-A.; formal analysis, J.L.M. and P.D.; writing—original draft preparation, J.L.M., M.E.L.-B., P.A.P.-A., P.D., M.A.M., D.H., J.G.-R., and D.A.Z. All authors have read and agreed to the published version of the manuscript.

**Funding:** This research received no external funding.

**Data Availability Statement:** The data presented in this study are available on request from the corresponding author.

**Conflicts of Interest:** The authors declare no conflict of interest.

## References

- Stephens, S.L.; Boerner, R.E.; Moghaddas, J.J.; Moghaddas, E.E.; Collins, B.M.; Dow, C.B.; Youngblood, A. Fuel treatment impacts on estimated wildfire carbon loss from forests in Montana, Oregon, California, and Arizona. *Ecosphere* **2012**, *3*, 1–17. [\[CrossRef\]](#)
- Pereira, P.; Francos, M.; Brevik, E.C.; Ubeda, X.; Bogunovic, I. Post-fire soil management. *Curr. Opin. Environ. Sci. Health* **2018**, *5*, 26–32. [\[CrossRef\]](#)
- Girardin, M.P.; Ali, A.A.; Carcaillet, C.; Gautgier, S.; Hély, C.; Le Goff, H.; Terrier, A.; Bergeron, Y. Fire in managed forest of eastern Canada: Risk and options. *For. Ecol. Manag.* **2013**, *294*, 238–249. [\[CrossRef\]](#)
- Versini, P.A.; Velasco, M.; Cabello, A.; Sempere-Torres, D. Hydrological impact of forest fires and climate change in Mediterranean basin. *Nat. Hazards* **2013**, *66*, 609–628. [\[CrossRef\]](#)
- MAPA. *Spain Los Incendios Forestales en España. 1 Enero–31 Diciembre 2018*; Avance Informativo Ministerio de Agricultura, Pesca y Alimentación, Gobierno de España: Madrid, Spain, 2019.
- Lachowski, H.; Hardwick, P.; Griffith, R.; Parsons, A.; Warbington, R. Faster, better data for burned watersheds needing emergency rehab. *J. For.* **1997**, *95*, 4–8.
- Moody, J.A.; Shakesby, R.A.; Robichaud, P.R.; Cannon, S.H.; Martin, D.A. Current research issues related to post-wildfire runoff and erosion processes. *Earth Sci. Rev.* **2013**, *122*, 10–37. [\[CrossRef\]](#)
- Zema, D.A.; Nunes, J.P.; Lucas-Borja, M.E. Improvement of seasonal runoff and soil loss predictions by the MMF (Morgan-Morgan-Finney) model after wildfire and soil treatment in Mediterranean forest ecosystems. *Catena* **2020**, *188*, 104415. [\[CrossRef\]](#)
- Ryu, S.R.; Choi, H.T.; Lim, J.H.; Lee, I.K.; Ahn, Y.S. Post-fire restoration plan for sustainable forest management in South Korea. *Forests* **2017**, *8*, 188. [\[CrossRef\]](#)
- Viana-Soto, A.; Aguado, I.; Martínez, S. Assessment of post-fire vegetation recovery using fire severity and geographical data in the mediterranean region (Spain). *Environments* **2017**, *4*, 90. [\[CrossRef\]](#)
- Robichaud, P.R.; Wagenbrenner, J.W.; Brown, R.E.; Wohlgemuth, P.M.; Beyers, J.L. Evaluating the effectiveness of contour-felled log erosion barriers as a post-fire runoff and erosion mitigation treatment in the western United States. *Int. J. Wildland Fire* **2008**, *17*, 255–273. [\[CrossRef\]](#)
- Fernández, C.; Fontúrbel, T.; Vega, J.A. Effects of pre-fire site preparation and post-fire erosion barriers on soil erosion after a wildfire in NW Spain. *Catena* **2019**, *172*, 691–698. [\[CrossRef\]](#)
- Badía, D.; Sánchez, C.; Aznar, J.M.; Martí, C. Post-fire hillslope log debris dams for runoff and erosion mitigation in the semiarid Ebro Basin. *Geoderma* **2015**, *237*, 298–307. [\[CrossRef\]](#)
- Wittenberg, L.; van der Wal, H.; Keesstra, S.; Tessler, N. Post-fire management treatment effects on soil properties and burned area restoration in a wildland-urban interface, Haifa Fire case study. *Sci. Total. Environ.* **2020**, *716*, 135190. [\[CrossRef\]](#)
- Niemeyer, R.J.; Bladon, K.D.; Woodsmith, R.D. Long-term hydrologic recovery after wildfire and post-fire forest management in the interior Pacific Northwest. *Hydrol. Process.* **2020**, *34*, 1182–1197. [\[CrossRef\]](#)
- Keith, H.; Lindenmayer, D.; Mackey, B.; Blair, D.; Carter, L.; McBurney, L.; Konishi-Nagano, T. Managing temperate forests for carbon storage: Impacts of logging versus forest protection on carbon stocks. *Ecosphere* **2014**, *5*, 1–34. [\[CrossRef\]](#)
- Raftoyannis, Y.; Spanos, I. Evaluation of log and branch barriers as post-fire rehabilitation treatments in a Mediterranean pine forest in Greece. *Int. J. Wildland Fire* **2005**, *14*, 183–188.

18. Robichaud, P.R. Fire effects on infiltration rates after prescribed fire in Northern Rocky Mountain forests, USA. *J. Hydrol.* **2000**, *231*, 220–229. [[CrossRef](#)]
19. Leverkus, A.B.; Rey Benayas, J.M.; Castro, J.; Boucher, D.; Brewer, S.; Collins, B.M.; Lee, E.-J. Salvage logging effects on regulating and supporting ecosystem services—A systematic map. *Can. J. For. Res.* **2018**, *48*, 983–1000. [[CrossRef](#)]
20. Lindenmayer, D.B.; Noss, R.F. Salvage logging, ecosystem processes, and biodiversity conservation. *Conserv. Biol.* **2006**, *20*, 949–958. [[CrossRef](#)] [[PubMed](#)]
21. Fox, D.M.; Maselli, F.; Carrega, P. Using SPOT images and field sampling for mapping burn severity and vegetation factors affecting post fire erosion risk. *Catena* **2008**, *75*, 326–335. [[CrossRef](#)]
22. Szpakowski, D.M.; Jensen, J.L. A review of the applications of remote sensing in fire ecology. *Remote. Sens.* **2019**, *11*, 2638. [[CrossRef](#)]
23. Alfonso-Torreño, A.; Gómez-Gutiérrez, Á.; Schnabel, S.; Contador, J.F.L.; de Sanjosé Blasco, J.J.; Fernández, M.S. sUAS, SfM-MVS photogrammetry and a topographic algorithm method to quantify the volume of sediments retained in check-dams. *Sci. Total. Environ.* **2019**, *678*, 369–382. [[CrossRef](#)] [[PubMed](#)]
24. Gitelson, A.A.; Stark, R.; Grits, U.; Rundquist, D.; Kaufman, Y.; Derry, D. Vegetation and soil lines in visible spectral space: A concept and technique for remote estimation of vegetation fraction. *Int. J. Remote. Sens.* **2002**, *23*, 2537–2562. [[CrossRef](#)]
25. Gitas, I.; Mitri, G.; Veraverbeke, S.; Polychronaki, A. Advances in remote sensing of post-fire vegetation recovery monitoring—A review. *Remote Sens. Biomass Princ. Appl.* **2012**, *1*, 334.
26. Bhagat, V.S.; Kadam, A.; Kumar, S. Analysis of Remote Sensing based Vegetation Indices (VIs) for Unmanned Aerial System (UAS): A Review. *Remote Sens. Land* **2019**, *3*, 58–73. [[CrossRef](#)]
27. Evangelides, C.; Nobajas, A. Red-Edge Normalised Difference Vegetation Index (NDVI705) from Sentinel-2 imagery to assess post-fire regeneration. *Remote Sens. Appl. Soc. Environ.* **2020**, *17*, 100283. [[CrossRef](#)]
28. Xue, J.; Su, B. Significant remote sensing vegetation indices: A review of developments and applications. *J. Sens.* **2017**, 1353691. [[CrossRef](#)]
29. Sirin, A.; Medvedeva, M.; Maslov, A.; Vozbrannaya, A. Assessing the Land and Vegetation Cover of Abandoned Fire Hazardous and Rewetted Peatlands: Comparing Different Multispectral Satellite Data. *Land* **2018**, *7*, 71. [[CrossRef](#)]
30. Bright, B.C.; Hudak, A.T.; Kennedy, R.E.; Braaten, J.D.; Khalyani, A.H. Examining post-fire vegetation recovery with Landsat time series analysis in three western North American forest types. *Fire Ecol.* **2019**, *15*, 1–14. [[CrossRef](#)]
31. Lentile, L.B.; Morgan, P.; Hudak, A.T.; Bobbitt, M.J.; Lewis, S.A.; Smith, A.M.; Robichaud, P.R. Post-fire burn severity and vegetation response following eight large wildfires across the western United States. *Fire Ecol.* **2007**, *3*, 91–108. [[CrossRef](#)]
32. Bastos, A.; Gouveia, C.; DaCamara, C.; Trigo, R. Landscape, fire distribution and vegetation recovery in Portugal: 2003 and 2005 fire seasons. In *Advances in Remote Sensing and GIS Applications in Forest Fire Management: From Local to Global Assessments*; EUR 24941 EN; Miguel-Ayanz, J., Camia, A., Gitas, I., Santos De Oliveira, S., Eds.; Publications Office of the European Union: Luxembourg, 2011; JRC66634.
33. Lasaponara, R.; Montesano, T.; Desantis, F.; Lanorte, A. Evaluating post fire vegetation recovery using satellite MODIS data. In *Advances in Remote Sensing and GIS Applications in Forest Fire Management: From Local to Global Assessments*; EUR 24941 EN; Miguel-Ayanz, J., Camia, A., Gitas, I., Santos De Oliveira, S., Eds.; Publications Office of the European Union: Luxembourg, 2011; JRC66634.
34. Polychronaki, A.I.; Gitas, I.Z.; Minchella, A. Monitoring post-fire vegetation recovery using optical and sar data. In *Advances in Remote Sensing and GIS Applications in Forest Fire Management: From Local to Global Assessments*; EUR 24941 EN; Miguel-Ayanz, J., Camia, A., Gitas, I., Santos De Oliveira, S., Eds.; Publications Office of the European Union: Luxembourg, 2011; JRC66634.
35. San-Miguel-Ayanz, J.; Camia, A.; Gitas, I.; Santos De Oliveira, S. (Eds.) *Advances in Remote Sensing and GIS Applications in Forest Fire Management: From Local to Global Assessments*; EUR 24941 EN; Publications Office of the European Union: Luxembourg, 2011; JRC66634.
36. Schneider, P.; Roberts, D.A.; Kyriakidis, P.C. A VARI-based relative greenness from MODIS data for computing the Fire Potential Index. *Remote. Sens. Environ.* **2008**, *112*, 1151–1167. [[CrossRef](#)]
37. Stow, D.; Niphadkar, M.; Kaiser, J. MODIS-derived visible atmospherically resistant index for monitoring chaparral moisture content. *Int. J. Remote. Sens.* **2005**, *26*, 3867–3873. [[CrossRef](#)]
38. Jiménez-Muñoz, J.C.; Sobrino, J.A.; Plaza, A.; Guanter, L.; Moreno, J.; Martínez, P. Comparison between fractional vegetation cover retrievals from vegetation indices and spectral mixture analysis: Case study of PROBA/CHRIS data over an agricultural area. *Sensors* **2009**, *9*, 768–793. [[CrossRef](#)]
39. Larrinaga, A.R.; Brotons, L. Greenness indices from a low-cost UAV Imagery as tools for monitoring post-fire forest recovery. *Drones* **2019**, *3*, 6. [[CrossRef](#)]
40. Christakopoulos, P.; Paronis, D.; Scarvelis, M.; Kalabokides, K.; Hatzopoulos, I. Comparative evaluation of restoration practices applied to mediterranean forest ecosystems using remote sensing and GIS: Natural regeneration versus reforestation. In *Advances in Remote Sensing and GIS Applications in Forest Fire Management: From Local to Global Assessments*; EUR 24941 EN; Miguel-Ayanz, J., Camia, A., Gitas, I., Santos De Oliveira, S., Eds.; Publications Office of the European Union: Luxembourg, 2011; JRC66634.
41. Rivas-Martínez, S.; Rivas-Saenz, S.; Penas, A. *Worldwide Bioclimatic Classification System*; Backhuys Pub: Leiden, The Netherlands, 2002.

42. State Meteorological Agency-AEMET-Spanish Government. Available online: <http://www.aemet.es/es/portada> (accessed on 12 January 2021).
43. IGN. *Mapa de Suelos de España*; Instituto Geográfico Nacional: Madrid, Spain, 2006.
44. Soil Survey Staff. *Keys to Soil Taxonomy*; Natural Resources Conservation Service—Department of Agriculture: Washington, DC, USA, 2014.
45. Napper, C. *Burned Area Emergency Response Treatments Catalog*; National Technology & Development Program, Watershed, Soil Air Management 0625 1801-SDTDC; USDA Forest Service: San Dimas, CA, USA, 2006.
46. Canfield, R. Application of Line Interception Method in Sampling Range Vegetation. *J. For.* **1941**, *39*, 388–394.
47. Zema, D.A.; Plaza-Alvarez, P.A.; Xu, X.; Carra, B.G.; Lucas-Borja, M.E. Influence of forest stand age on soil water repellency and hydraulic conductivity in the Mediterranean environment. *Sci. Total. Environ.* **2020**, *753*, 142006. [[CrossRef](#)]
48. Zema, D.A.; Van Stan, J.T.; Plaza-Alvarez, P.A.; Xu, X.; Carra, B.G.; Lucas-Borja, M.E. Effects of stand composition and soil properties on water repellency and hydraulic conductivity in Mediterranean forests. *Ecohydrology* **2021**, *14*, e2276. [[CrossRef](#)]
49. Millar, R.B.; Anderson, M.J. Remedies for pseudoreplication. *Fish. Res.* **2004**, *70*, 397–407. [[CrossRef](#)]
50. Wu, J.; Yang, Q.; Li, Y. Partitioning of Terrain Features Based on Roughness. *Remote Sens.* **2018**, *10*, 1985. [[CrossRef](#)]
51. Halthore, R.N.; Markham, B.L. Overview of atmospheric correction and radiometric calibration efforts during FIFE. *J. Geophys. Res. Atmos.* **1992**, *97*, 18731–18742. [[CrossRef](#)]
52. Keeley, J.E.; Pausas, J.G. Distinguishing disturbance from perturbations in fire-prone ecosystems. *Int. J. Wildland Fire* **2019**, *28*, 282–287. [[CrossRef](#)]
53. Gómez-Sánchez, E.; Lucas-Borja, M.E.; Plaza-Alvarez, P.A.; González-Romero, J.; Sagra, J.; Moya, D.; De las Heras, J. Effects of postfire hillslope stabilisation techniques on chemical, physico-chemical and microbiological soil properties in Mediterranean forest ecosystems. *J. Environ. Manag.* **2019**, *246*, 229–238. [[CrossRef](#)] [[PubMed](#)]
54. Albert-Belda, E.; Bermejo-Fernández, A.; Cerdà, A.; Taguas, E.V. The use of Easy-Barriers to control soil and water losses in fire-affected land in Quesada, Andalusia, Spain. *Sci. Total. Environ.* **2019**, *690*, 480–491. [[CrossRef](#)] [[PubMed](#)]
55. Jourgholami, M.; Ahmadi, M.; Tavankar, F.; Picchio, R. Effectiveness of Three Post-Harvest Rehabilitation Treatments for Runoff and Sediment Reduction on Skid Trails in the Hyrcanian Forests. *Croat. J. For. Eng. J. Theory Appl. For. Eng.* **2020**, *41*, 1–16. [[CrossRef](#)]
56. Eng, L.S.; Ismai, R.; Hashim, W.; Mohamed, R.R.; Baharum, A. Vegetation monitoring using UAV: A preliminary Study. *Int. J. Eng. Technol.* **2018**, *7*, 223–227. [[CrossRef](#)]
57. Cermakova, I.; Komarkova, J.; Sedlak, P. Calculation of visible spectral indices from UAV-based data: Small water bodies monitoring. In Proceedings of the 14th Iberian Conference on Information Systems and Technologies (CISTI), Coimbra, Portugal, 19–22 June 2019; pp. 1–5.
58. Themistocleous, K. DEM Modeling using RGB-based vegetation indices from UAV images. *Proc. SPIE* **2019**, 11174. [[CrossRef](#)]
59. Fathipoor, H.; Arefi, H.; Shah-Hosseini, R.; Moghadam, H. Corn forage yield prediction using unmanned aerial vehicle images at mid-season growth stage. *J. Appl. Remote Sens.* **2019**, *13*, 034503. [[CrossRef](#)]
60. Wan, L.; Li, Y.; Cen, H.; Zhu, J.; Yin, W.; Wu, W.; Zhu, H.; Sun, D.; Zhou, W.; He, Y. Combining UAV-based vegetation indices and image classification to estimate flower number in oilseed rape. *Remote Sens.* **2018**, *10*, 1484. [[CrossRef](#)]
61. Mokarram, M.; Bolorani, A.D.; Hojati, M. Relationship between Land Cover and Vegetation Indices. Case Study: Eghlid Plain, Fars Province, Iran. *Eur. J. Geogr.* **2016**, *7*, 48–60.
62. Mokarram, M.; Hojjati, M.; Roshan, G.; Negahban, S. Modeling the Behavior of Vegetation Indices in the Salt Dome of Korsia in North-East of Darab, Fars, Iran. *Modeling Earth Syst. Environ.* **2015**, *1*, 1–9. [[CrossRef](#)]
63. Corona, P.; Lamónaca, A.; Chirici, G. Remote sensing support for post fire forest management. *Ifor. Biogeosci. For.* **2008**, *1*, 6. [[CrossRef](#)]
64. Fernández-Guisuraga, J.M.; Sanz-Ablanedo, E.; Suárez-Seoane, S.; Calvo, L. Using unmanned aerial vehicles in postfire vegetation survey campaigns through large and heterogeneous areas: Opportunities and challenges. *Sensors* **2018**, *18*, 586. [[CrossRef](#)] [[PubMed](#)]
65. Hou, T.; Filley, T.R.; Tong, Y.; Abban, B.; Singh, S.; Papanicolaou, A.T.; Wacha, K.M.; Wilson, C.G.; Chaubey, I. Tillage-induced surface soil roughness controls the chemistry and physics of eroded particles at early erosion stage. *Soil Tillage Res.* **2021**, *207*, 104807. [[CrossRef](#)]
66. Römken, M.J.; Helming, K.; Prasad, S.N. Soil erosion under different rainfall intensities, surface roughness, and soil water regimes. *Catena* **2002**, *46*, 103–123. [[CrossRef](#)]
67. Govers, G.; Takken, I.; Helming, K. Soil roughness and overland flow. *Agronomie* **2000**, *20*, 131–146. [[CrossRef](#)]
68. De Almeida, W.S.; Panachuki, E.; de Oliveira, P.T.S.; da Silva Menezes, R.; Sobrinho, T.A.; de Carvalho, D.F. Effect of soil tillage and vegetal cover on soil water infiltration. *Soil Tillage Res.* **2018**, *175*, 130–138. [[CrossRef](#)]
69. Nunes, J.P.; Bernard-Jannin, L.; Rodriguez Blanco, M.L.; Santos, J.M.; Coelho, C.D.O.A.; Keizer, J.J. Hydrological and erosion processes in terraced fields: Observations from a humid Mediterranean region in northern Portugal. *Land Degrad. Dev.* **2018**, *29*, 596–606. [[CrossRef](#)]
70. Meena, R.S.; Lal, R.; Yadav, G.S. Long-term impacts of topsoil depth and amendments on soil physical and hydrological properties of an Alfisol in central Ohio, USA. *Geoderma* **2020**, *363*, 114164. [[CrossRef](#)]
71. Zema, D.A. Post-fire management impacts on soil hydrology. *Curr. Opin. Environ. Sci. Health* **2021**, *21*, 100252. [[CrossRef](#)]